A coarse-to-fine approach for efficient deformation of curved high-order meshes

Hemant Chaurasia[1], Xevi Roca[1], Per-Olof Persson[2] and Jaime Peraire[1]

[1] Massachusetts Institute of Technology, Cambridge, MA, USA hemantc@mit.edu, xeviroca@mit.edu, peraire@mit.edu
[2] University of California, Berkeley, CA, USA persson@berkeley.edu

1 Introduction

We propose a coarse-to-fine approach for generating fine and curved high-order tetrahedral meshes. The proposed approach is performed in three steps: (1) generate a coarse reference mesh; (2) map this to a coarse and curved high-order mesh; and (3) refine the curved high-order mesh. The approach provides high-order meshes that are valid, have the desired interpolation degree, and can be computed with a greatly reduced computational cost. Moreover, it enables the direct conversion of isotropic meshes (*e.g.* an Euler mesh) into anisotropic meshes (*e.g.* a Navier-Stokes boundary layer mesh).

The key application of this method is to generate sequences of large-amplitude deformed meshes over time. These mesh sequences are required for high-order simulations with time-dependent geometries, such as in fluid dynamic simulations of flapping wings using the Arbitrary Lagrangian-Eulerian method [1]. For these problems, a reference mesh is typically deformed to accommodate several different wing configurations. To this end, a Lagrangian solid mechanics equation is solved on the same mesh, taking the wing displacement state as a Dirichlet boundary condition [2]. Generating fine deformed meshes in this manner is expensive since flow simulations of flapping wings often require $\sim 10^5$ high-order elements, including the highly refined regions in the boundary layer. With our approach, the number of degrees of freedom required to perform mesh deformation can be reduced more than 500 times.

In the sections that follow, we describe further details of our methodology (Section 2), an application of our method to the meshing problem for a 3D flapping bat wing (Section 3), and concluding remarks (Section 4).

2 Methodology

Our goal is to generate fine and curved high-order meshes that conform to a curved boundary that is moving in time. Moreover, the final mesh has to

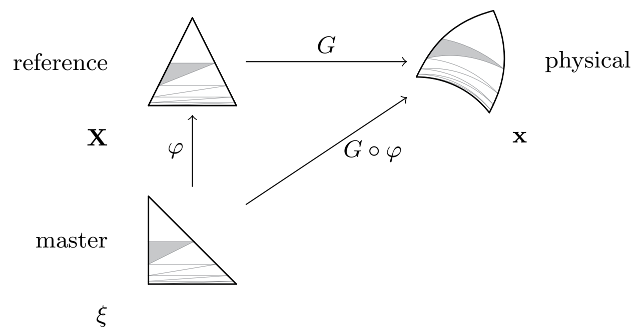

Fig. 1. Mappings between the master, reference and physical domains. Representation of the coarse (black) and fine (grey) elements.

present the prescribed isotropic and anisotropic refinement features. To this end, we propose the following approach (Figure 1):

1. Generate a coarse and straight-sided reference mesh. We generate a coarse linear mesh for a fixed boundary configuration. Then, we convert this linear mesh to a high-order mesh with straight-sided faces. Thus, the reference elements are the image of an invertible affine mapping φ from a high-order and straight-sided master element (coordinates ξ) to the reference space (coordinates $\mathbf{X}$), as shown in Figure 1. Note that the affine mapping φ is invertible if and only if $\det\nabla_{\xi}\varphi$ is non-zero.

2. Generate coarse and curved physical meshes over time. We seek a coarse mesh on the physical domain (coordinates $\mathbf{x}$) composed of high-order elements positively oriented and with curved sides that conform to the boundary data. Specifically, we seek a smooth deformation G from the reference to the physical space that is also a *diffeomorphism* (differentiable and invertible), as shown in Figure 1. Note that if the boundary does not present self-intersections, this is equivalent to requiring that $\det\nabla_{\mathbf{X}}G$ is positive everywhere. To find the deformation G we use the non-linear elasticity approach for curved mesh generation proposed in [1].

3. Refine the coarse and curved physical meshes over time. For each physical element to be refined, we select the required refinement template (uniform, boundary layer, ...). As illustrated in Figure 1, all the templates are determined by a refinement of the master element (black) with straight-sided sub-elements (grey). Then, the sub-elements in the master element (grey) are mapped to the corresponding coarse reference elements (black) by means of the affine mapping φ. This results in a fine and high-order reference mesh composed of straight-sided elements (grey). Finally, the fine reference mesh is mapped to the physical space by means of the diffeomorphism G. The resulting refined and curved high-order mesh (grey) is the desired mesh. Note that the elements of this mesh are embedded inside the coarse and curved high-order physical elements.

Advantages. The proposed methodology provides a fine physical mesh that: is valid; has the same interpolation degree (k) as the master and reference elements; and is cheap to compute. First, the physical elements are valid since they are the image of the smooth diffeomorphism $G \circ \varphi$ from the refined master element to the physical domain. Note that $G \circ \varphi$ is a smooth diffeomorphism because it is the composition of the smooth diffeomorphisms φ (invertible affine mapping) and G (invertible deformation). Second, the physical elements have interpolation degree k since $G \circ \varphi$ is the composition of a mapping φ of linear degree (affine) and a deformation mapping G of k^{th} degree (by construction). Third, the proposed approach is cheaper than computing directly the deformations on the fine meshes. That is, the cost of the process is dominated by the generation of the coarse and curved high-order physical mesh. The cost of the refinement is negligible since it corresponds to refining the master element and using the mapping $G \circ \varphi$ to interpolate the physical coordinates of the nodes of the fine physical mesh.

3 Application: flapping bat wing

Problem description. Here we show an application of our method to the mesh generation problem for high-order fluid dynamic simulations of a 3D flapping bat wing. Kinematic data for the bat surface is provided as a function of time and used as the Dirichlet boundary condition for a series of very large amplitude mesh deformation calculations. The simulations require high-order meshes with anisotropic boundary layer refinement in regions adjacent to the wing.

Reference mesh design. The first step in our methodology is to generate a coarse isotropic high-order mesh for a reference configuration of the boundary surface. Special attention was paid to reduce the stiffness determined by the mesh topology, particularly between the two wings. To this end, we have generated a mesh where each edge on the wing surface is shared by at least six elements (three above and three below). This helps to ensure that the mesh deformation solver converges through the large range of motion of the bat wing. The reference mesh contains 2,016 2^{nd}-order elements, which is sufficient to resolve the boundary geometry in this problem.

Mesh deformation results. Following our procedure, a sequence of 333 boundary-conforming deformed meshes was computed from the reference mesh for the wing's full range of motion. Examples of these deformed meshes are presented in Figure 2. The quality of these deformed meshes is quantified in Figure 3. We show the minimum value at each time instance for the scaled Jacobian measure I [3], and the extension of the shape measure to high-order elements Q [4].

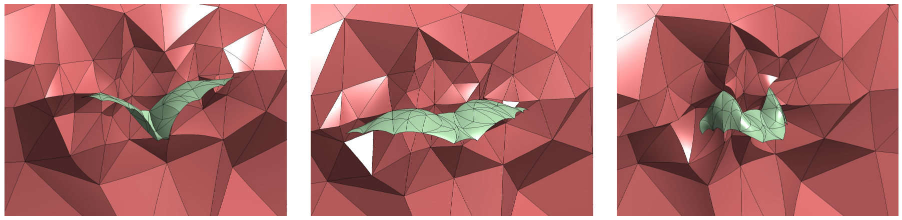

Fig. 2. Deformation of a coarse volume mesh near the front of a flapping bat wing.

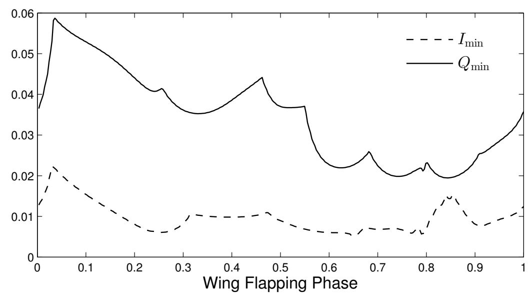

Fig. 3. Minimum quality for a sequence of deformed meshes of a flapping bat wing.

Mesh refinement results. The coarse deformed meshes define a diffeomorphism mapping between the reference mesh and the deformed mesh, via an isoparametric mapping in this case. Together with the mapping, we used a set of isotropic and anisotropic mesh refinement templates to generate the refined mesh in Figure 4. This refined mesh was generated for all deformation states using the coarse mesh results, at negligible computational cost.

The refined mesh meets the requirements for an anisotropic boundary layer and wake region. This example has 56,989 3$^{\text{rd}}$-order elements, in contrast to the 2,016 2$^{\text{nd}}$-order elements used in the coarse reference mesh. Even for this modest degree of refinement, our approach reduces the number of degrees of freedom required for the mesh deformation computation by a factor of 56, resulting in significantly lower computational cost.

4 Concluding Remarks

We have presented a coarse-to-fine approach for generating fine and curved high-order tetrahedral meshes. The approach provides high-order meshes that are valid, have the desired interpolation degree, and can be computed with a reduced computational cost. Moreover, the approach enables the construction of a Navier-Stokes boundary layer mesh from an isotropic Euler mesh. A key application of this method is to generate sequences of large-amplitude deformed meshes over time for flow simulations of flapping wings. With the

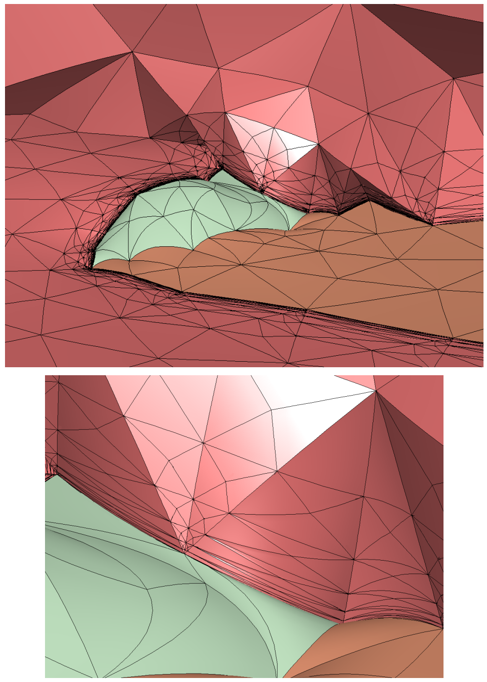

Fig. 4. Cross section of bat mesh showing boundary layer and wake refinement.

proposed approach the number of degrees of freedom required to perform the deformation can be reduced more than 500 times.

Acknowledgements. The authors would like to acknowledge support for this work provided by the AFOSR MURI on Bio-Inspired Flight for Micro Air Vehicles. Special thanks to our MURI collaborators at Brown University for supplying bat flight kinematic data.

References

1. P.-O. Persson, J. Bonet, and J. Peraire. Discontinuous Galerkin solution of the Navier-Stokes equations on deformable domains. *Computer Methods in Applied Mechanics and Engineering*, 198(17-20):1585 – 1595, 2009.
2. P.-O. Persson and J. Peraire. Curved mesh generation and mesh refinement using lagrangian solid mechanics. In *Proc. of the 47th AIAA Aerospace Sciences Meeting and Exhibit*, 2009. AIAA-2009-949.
3. S. Dey, R. O'Bara, and M. Shephard. Curvilinear mesh generation in 3d. *Comput. Aided Geom. Design*, 33:199–209, 2001.
4. X. Roca, A. Gargallo-Peiró, and J. Sarrate. Defining quality measures for high-order planar triangles and curved mesh generation. In *Proceedings of the 20th International Meshing Roundtable*, pages 365–383, 2011.